Bioinorganic Chemistry

A Combined NRVS and DFT Study of Fe^{IV}=O Model Complexes: A Diagnostic Method for the Elucidation of Non-Heme Iron Enzyme Intermediates**

Caleb B. Bell, III, Shaun D. Wong, Yuming Xiao, Eric J. Klinker, Adam L. Tenderholt, Matt C. Smith, Jan-Uwe Rohde, Lawrence Que, Jr., Stephen P. Cramer, and Edward I. Solomon

Fe^{IV}=O intermediates have been shown to be key catalytic species in a growing number of mononuclear non-heme iron (NHI) enzymes. Various combinations of Mössbauer (Mb), electron–nuclear double resonance, magnetic circular dichroism (MCD), and extended X-ray absorption spectroscopy data exist on these species, providing electronic insight into and bonding descriptions of the Fe^{IV}=O unit.[1] However, information regarding other chemically important features necessary for mechanistic insight (overall structure) is mostly lacking. Resonance Raman (rR) and IR spectroscopy can, in principle, provide such insight, but owing to selection rules, low absorption intensities (NHI species lack the intense Soret band), and other factors, experimental data are limited.[2] Herein, we present vibrational data obtained by nuclear resonance vibrational spectroscopy (NRVS) on three Fe^{IV}=O complexes interpreted by coupling with DFT calculations, with particular focus on understanding the low-energy spectral region. The data show systematic trends that provide molecular-level insight reflecting the Fe^{IV} ligand environment and reactivity. Computationally, these studies are extended to models of the Fe^{IV}=O species in the NHI enzymes HmaS and HPPD (see below) and show that Fe^{IV} species can be experimentally differentiated using NRVS.

The NRVS experiment employs synchrotron radiation tuned to the 14.4 keV ^{57}Fe nuclear Mb transition.[3–5] Inelastic

scattering, where phonon annihilation and creation events couple with nuclear excitation, yields the Fe partial vibrational density of states (PVDOS) NRVS spectrum. This is analogous to Stokes and anti-Stokes rR scattering, but NRVS intensity is gained through Fe displacement (ΔFe), via the mode composition factor, and provides selective enhancement of all Fe core modes with no background.[6] This method has been applied to iron–sulfur and heme enzymes, nitrogenase, and model complexes.[7–16] NRVS data for an Fe^{V} nitrido complex with a ligand similar to that in **1** (see below) have been reported.[16] However, detailed analysis in the low-energy region was complicated by inhomogeneity in the sample.[16]

Fe^{IV}=O ($S=1$) functional models have been synthesized with 1,4,8,11-tetramethyl-1,4,8,11-tetraazacyclotetradecane (**1**); *N,N*-bis(2-pyridylmethyl)-*N*-bis(2-pyridyl)methylamine (**2**); and *N*-benzyl-*N,N′,N′*-tris(2-pyridylmethyl)-1,2-diaminoethane (**3**) ligands.[17–19] Each complex is six-coordinate: **1** has an equatorial (eq) ring with tertiary amines and an axial (ax) $NCCH_3$ ligand; **2** has eq pyridyl ligands (py) and a tethered ax tertiary amine, and **3** is quite rhombic, with two tertiary amine and three py ligands. Structures are available for **1** and **2**. Note, **2** and **3** are more reactive than **1** in their ability to H-atom abstract from cyclohexane.[20]

The NRVS data for **1**, **2**, and **3** are shown in Figure 1. Isotope-sensitive peaks are observed at 831 (796 in ^{18}O), 820 (788), and 824 (786) cm^{-1} that can be assigned as ν_2, the FeO stretch (normal modes in Figure 2).[21,22] Resolution on NRVS energies is 8 cm^{-1}. These energies correlate well with the calculated energies and isotope shifts (see the Supporting Information, Figure S2). This mode has been observed only in **1** at 834 cm^{-1} by IR spectroscopy and at 839 cm^{-1} by rR spectroscopy, in good agreement with our results.[19,23] The comparable energies of ν_2, given the resolution of the NRVS experiment, imply that the total FeO bonding in these complexes are similar. Excited-state MCD data have shown the FeO π bond is stronger in **2** than in **1**; therefore, the σ bond must be weaker.[24] This conclusion can be rationalized by considering the stronger donation of the eq ligands in **2** (see below), which donate into the donut of the d_{z^2} orbital and compete with the oxo ligand for σ bonding.

Moving down in energy, a weak peak is observed at 653 cm^{-1} in **2** and **3**, while for **1** the next resolvable peak is at 526 cm^{-1}. In **2** and **3** this peak is assigned, based on DFT calculations, as ν_8, the asymmetric FeN_{eq} stretches. In the calculations, these are shifted to the 450–470 cm^{-1} region in **1** and are not resolved in the data. In total, four modes involve

[*] C. B. Bell, III, S. D. Wong, A. L. Tenderholt, Prof. E. I. Solomon
Department of Chemistry, Stanford University
Stanford, CA 94305-5080 (USA)
Fax: (+1) 650-725-0259
E-mail: Edward.Solomon@stanford.edu

Dr. Y. Xiao, Dr. M. C. Smith, Prof. S. P. Cramer
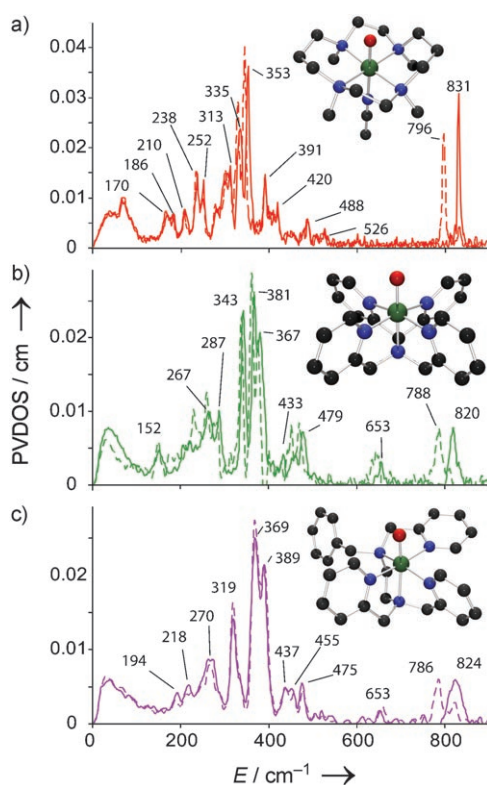Department of Applied Science, University of California, Davis
and
Physical Biosciences Division, Lawrence Berkeley National Laboratory (USA)

Dr. E. J. Klinker, Dr. J.-U. Rohde, Prof. L. Que, Jr.
Department of Chemistry, University of Minnesota (USA)

Supporting information for this article is available on the WWW under http://dx.doi.org/10.1002/anie.200803740.

WILEY
InterScience®
DISCOVER SOMETHING GREAT

Figure 1. NRVS PVDOS for a) **1**, b) **2**, and c) **3** with ^{16}O (solid lines) and ^{18}O (dotted lines); insets show the 3D structures of complexes.
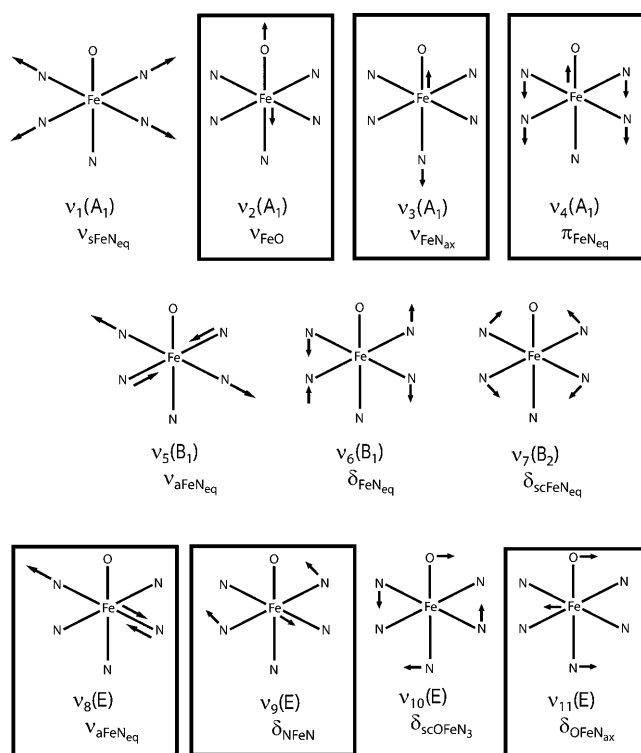
Figure 2. Normal modes for C_{4v} complexes adapted from reference [21]. Modes with ΔFe are boxed. Nomenclature follows that of Nakamoto.[22]

FeN$_{eq}$ stretching (including the NRVS-inactive ν_1 and ν_5) and probe eq bonding; the average energy of these sets is 355, 648, and 598 cm^{-1}, respectively. Calculations where the eq ring in **1** is cleaved (**1′**, see the Supporting Information) show that the average FeN bond length decreases by 0.07 Å, the splitting of the four modes decreases, and the average energy increases to 430 cm^{-1}. These results show that the chelate in **1** influences the eq bonding but that the overall bond strength is determined by the greater σ donation of the py ligands relative to tertiary amines, which affects FeO bonding.

Continuing down in energy, the first intense feature is assigned as ν_3 (FeN$_{ax}$ stretch) at 391, 367, and 389 cm^{-1}, in **1**, **2**, and **3**, respectively. In the calculations, these bands show variable intensity (bars in Figure 3) and mix with ν_{11}. The
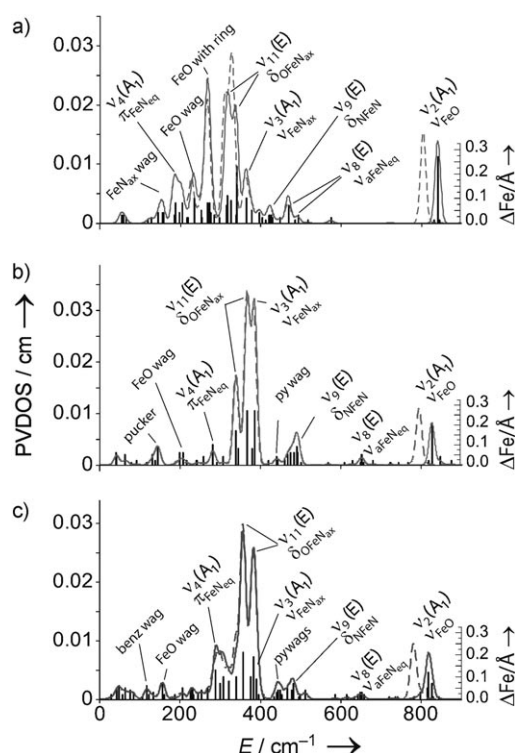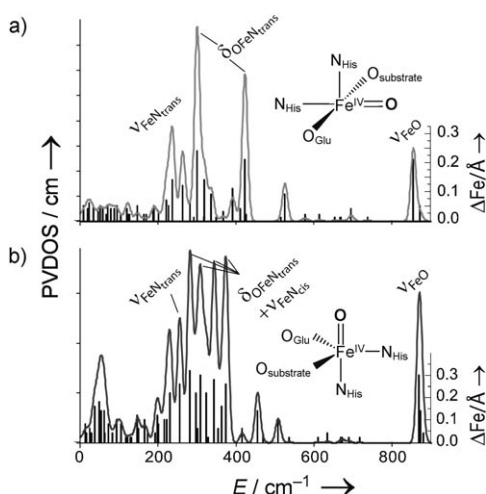

Figure 3. DFT calculated NRVS PVDOS for a) **1**, b) **2**, and c) **3** (^{16}O (solid lines) and ^{18}O (dotted lines)) with ΔFe included as bars.

resulting ΔFe has both in-plane (ip) and out-of-plane (op) contributions from ν_{11} and ν_3. The ip motion in **1** is restricted by the chelate, thus reducing ΔFe, and consequently intensity. In **1′**, ΔFe is restored and ν_3 shifts to 294 cm^{-1} (Figure S4 in the Supporting Information). Calculations where the ax tether is removed in **2** (**2′**, see the Supporting Information) show that ν_3 is shifted down in energy to 300 cm^{-1}, consistent with a 0.05 Å increase of the FeN$_{ax}$ bond length, but the ip and op ΔFe are preserved. This mode reflects the bond *trans* to the oxo and constraints in the ligand environment.

The remaining two intense features are assigned as $\nu_{11a/b}$ (OFeN$_{ax}$ bends), which are split due to orthogonal differences in the eq ligand environment and to ring size in **1**, ax tether in **2**, and eq chelate in **3**. The splitting is 50 cm^{-1} in **3** but only approximately 25 cm^{-1} in **1** and **2**, reflecting the contracted eq

chelate between a pair of *cis* nitrogen atoms in **3**, and affords a probe of rhombic (perpendicular to the FeO bond) distortion. In **1′**, the most symmetric model, the splitting is 6 cm^{-1}. In **2′** (where the *x* and *y* axes are still inequivalent), the energy positions and splitting are unchanged, but the calculated intensity is reduced because of increased N$_{ax}$ motion. The splitting of ν_{11} reflects the ligand environment perpendicular to the FeO bond and, combined with high intensity, should provide structural insight for Fe^{IV}=O intermediates.

(4-Hydroxyphenyl)pyruvate dioxygenase (HPPD) and (4-hydroxy)mandelate synthase (HmaS) are NHI enzymes containing a 2-His-1-Glu facial triad and use the same substrate ((4-hydroxyphenyl)pyruvate, HPP) but exhibit different reaction mechanisms (electrophilic aromatic attack and H-atom abstraction, respectively) dependent on the orientation of HPP in the protein pocket.[25] The first step in both reactions is decarboxylation of HPP, and computational studies on the resultant Fe^{IV}=O site show that two 5C geometries are reasonable: square pyramidal (sqp, **4**) with the oxo ligand in the eq plane, and trigional bipyramidal (tbp) with the oxo ligand axial (**5**).[25] DFT calculations show that NRVS can discriminate between these proposed structures. The calculated PVDOS are shown in Figure 4. The intense

Figure 4. DFT calculated NRVS PVDOS for **4** and **5**, with ΔFe included as bars.

peaks at 301 and 424 cm^{-1} in **4** are bends of the OFeN$_{trans}$ unit (*trans* to the oxo ligand) reminiscent of $\nu_{11a/b}$, where the large splitting arises from loss of the *cis* ligand. Intense peaks are also at 237 and 837 cm^{-1} which involve FeN$_{trans}$ (reminiscent of ν_3) and FeO (reminiscent of ν_2) stretches. For **1**, **2**, and **3**, ν_3 was observed at a higher energy than ν_{11}; the shift to lower energy in **4** is due to the increased effective mass of histidine. The NRVS data of **5** are distinctly different and can be understood considering the normal modes for a tbp complex (Figure S6 in the Supporting Information). The degenerate ν_6 and ν_7 pairs involve *trans* ax bends and *cis* metal–ligand stretches. These are highly mixed in **5** and produce four peaks with similar intensity. The *trans* N$_{His}$ stretch (reminiscent of ν_3) is also intense at 257 cm^{-1}. In summary, with the exception of the FeO stretch, the intense modes occur at low energies and,

because of the inverse energy dependence of NRVS intensity, these are likely to be detectable in enzyme intermediates and afford a mechanism for structural characterization.

Analysis of the ground-state NRVS vibrational data coupled with excited-state data from previous MCD studies provides detailed bonding descriptions of **1**, **2**, and **3**.[24,26] The increased reactivity of **2** and **3** relative to **1** correlates with the strength of the FeO π bond (oxo p character in the π* LUMO, the frontier molecular orbital) and is determined by equatorial ligand σ donation. Additionally, the ν_3 and ν_{11} modes show systematic trends that reflect the ligand environment. Lower-energy modes have generally not been used for geometric insight, but in NRVS spectra these are enhanced in intensity relative to higher-energy stretches (e.g. characteristic metal–ligand modes such as ν_{FeO}) and are more likely to be detected in intermediates. This study uses these modes for electronic structural insight on Fe^{IV}=O models and computationally evaluates their utility for determination of active site structure in NHI enzyme intermediates.

Experimental Section

[1] See Fe^{IV} special edition of *J. Inorg. Biochem.* **2006**, *100*, and references therein.

[2] D. A. Proshlyakov, T. F. Henshaw, G. R. Monterosso, M. J. Ryle, R. P. Hausinger, *J. Am. Chem. Soc.* **2004**, *126*, 1022.

[3] W. Sturhahn, *J. Phys. Condens. Matter* **2004**, *16*, S497.

[4] W. R. Scheidt, S. M. Durbin, J. T. Sage, *J. Inorg. Biochem.* **2005**, *99*, 60.

[5] R. Rüffer, A. I. Chumakov, *Hyperfine Interact.* **2000**, *128*, 255.

[6] E. E. Alp, T. M. Mooney, T. Toellner, W. Sturhahn, *Hyperfine Interact.* **1994**, *90*, 323.

[7] Y. Xiao, H. Wang, S. J. George, M. C. Smith, M. W. Adams, F. E. Jenney, Jr., W. Sturhahn, E. E. Alp, J. Zhao, Y. Yoda, A. Dey, E. I. Solomon, S. P. Cramer, *J. Am. Chem. Soc.* **2005**, *127*, 14596.

[8] B. M. Leu, M. Z. Zgierski, G. R. Wyllie, W. R. Scheidt, W. Sturhahn, E. E. Alp, S. M. Durbin, J. T. Sage, *J. Am. Chem. Soc.* **2004**, *126*, 4211.

[9] K. Achterhold, W. Sturhahn, E. E. Alp, F. G. Parak, *Hyperfine Interact.* **2002**, *141–142*, 3.

[10] Y. Xiao, M. L. Tan, T. Ichiye, H. Wang, Y. Guo, M. C. Smith, J. Meyer, W. Sturhahn, E. E. Alp, J. Zhao, Y. Yoda, S. P. Cramer, *Biochemistry* **2008**, *47*, 6612.

[11] Y. Xiao, K. Fisher, M. C. Smith, W. E. Newton, D. A. Case, S. J. George, H. Wang, W. Sturhahn, E. E. Alp, J. Zhao, Y. Yoda, S. P. Cramer, *J. Am. Chem. Soc.* **2006**, *128*, 7608.

[12] B. K. Rai, S. M. Durbin, E. W. Prohofsky, J. T. Sage, G. R. Wyllie, W. R. Scheidt, W. Sturhahn, E. E. Alp, *Biophys. J.* **2002**, *82*, 2951.

[13] B. K. Rai, S. M. Durbin, E. W. Prohofsky, J. T. Sage, M. K. Ellison, A. Roth, W. R. Scheidt, W. Sturhahn, E. E. Alp, *J. Am. Chem. Soc.* **2003**, *125*, 6927.

[14] B. K. Rai, E. W. Prohofsky, S. M. Durbin, *J. Phys. Chem. B* **2005**, *109*, 18983.

[15] S. Cramer, Y. Xiao, H. Wang, Y. Guo, M. Smith, *Hyperfine Interact.* **2007**, *170*, 47.

[16] T. Petrenko, S. DeBeer George, N. Aliaga-Alcalde, E. Bill, B. Mienert, Y. Xiao, Y. Guo, W. Sturhahn, S. P. Cramer, K. Wieghardt, F. Neese, *J. Am. Chem. Soc.* **2007**, *129*, 11053.

[17] E. J. Klinker, J. Kaizer, W. W. Brennessel, N. L. Woodrum, C. J. Cramer, L. Que, Jr., *Angew. Chem.* **2005**, *117*, 3756; *Angew. Chem. Int. Ed.* **2005**, *44*, 3690.

[18] J. U. Rohde, S. Torelli, X. Shan, M. H. Lim, E. J. Klinker, J. Kaizer, K. Chen, W. Nam, L. Que, Jr., *J. Am. Chem. Soc.* **2004**, *126*, 16750.

[19] J. U. Rohde, J. H. In, M. H. Lim, W. W. Brennessel, M. R. Bukowski, A. Stubna, E. Münck, W. Nam, L. Que, Jr., *Science* **2003**, *299*, 1037.

[20] J. Kaizer, E. J. Klinker, N. Y. Oh, J. U. Rohde, W. J. Song, A. Stubna, J. Kim, E. Munck, W. Nam, L. Que, Jr., *J. Am. Chem. Soc.* **2004**, *126*, 472.

[21] W. Preetz, D. Ruf, D. Tensfeldt, *Z. Naturforsch. B* **1984**, *39*, 1100.

[22] K. Nakamoto, *Infrared and Raman Spectra of Inorganic and Coordination Compounds*, Wiley, New York, **1997**.

[23] T. A. Jackson, J. U. Rohde, M. S. Seo, C. V. Sastri, R. DeHont, T. Ohta, T. Kitagawa, E. Munck, L. Que, Jr., *J. Am. Chem. Soc.* **2008**, *130*, 12394.

[24] A. Decker, J. U. Rohde, L. Que, Jr., E. I. Solomon, *J. Am. Chem. Soc.* **2004**, *126*, 5378.

[25] M. L. Neidig, A. Decker, O. W. Choroba, F. Huang, M. Kavana, G. R. Moran, J. B. Spencer, E. I. Solomon, *Proc. Natl. Acad. Sci. USA* **2006**, *103*, 12966.

[26] A. Decker, J. U. Rohde, E. J. Klinker, S. D. Wong, L. Que, Jr., E. I. Solomon, *J. Am. Chem. Soc.* **2007**, *129*, 15983.

[27] W. Sturhahn, *Hyperfine Interact.* **1995**, *95*, 6.

[28] W. Sturhahn, *Hyperfine Interact.* **2000**, *125*, 149.